

# Energy Transfer Process in $\text{MgF}_2 : \text{Gd}^{3+}, \text{Eu}^{3+}$ Phosphor : Application to Visible Quantum Cutting

S. R. Jaiswal<sup>\*1</sup>, P. A. Nagpure<sup>2</sup>, S. K. Omanwar<sup>3</sup>

<sup>1</sup> Department of Physics, Shri R.L.T. College of Science, Akola, Maharashtra, India

<sup>2</sup> Department of Physics, ShriShivaji Science College, Amravati, Maharashtra, India

<sup>3</sup> Department of Physics, SantGadge Baba Amravati University, Amravati, Maharashtra, India

## ABSTRACT

Visible quantum cutting (QC) is observed in  $\text{MgF}_2$  Co-doped with  $\text{Gd}^{3+}, \text{Eu}^{3+}$  phosphor synthesis via wet chemical method. Powder X-ray diffraction analysis shows structural purity. The emission and excitation spectra of  $\text{MgF}_2:\text{Gd}^{3+}, \text{Eu}^{3+}$  were investigated using the VUV beam line of the Beijing Synchrotron Radiation Facility (BSRF). Energy transfer in gadolinium compounds from the  $\text{Gd}^{3+}$  ions to  $\text{Eu}^{3+}$  through cross relaxation occurs in this process. Quantum efficiency was found to be greater than 100% under the excitation of 172 nm and 203 nm corresponding  $^8S_{7/2} \rightarrow ^6G_7$  transition of  $\text{Gd}^{3+}$  ions. The synthesized phosphor material is potential candidates for the applications of plasma display panel and mercury free fluoresce lamps.

**Keywords :** Quantum Cutting, Plasma Display Panels (PDPs), VUV Spectroscopy

## I. INTRODUCTION

For the development of mercury free florescent lamps and plasma display panels (PDPs), we require phosphor having quantum efficiency is greater than unity under VUV excitation. The phosphors having quantum efficiency is greater than unity are called quantum cutting phosphors. Quantum cutting provides a means to obtain two or more low energy photons for each high energy absorbed photon. Therefore it serves as a down converting (DC) mechanism with quantum efficiency greater than unity and it offers the prospect of providing enhanced energy effectiveness in lighting devices [1]. In order to obtain quantum-cutting phosphors with quantum efficiencies exceeding unity, the lanthanide ions are obvious candidates for this purpose due to their energy level structures that afford metastable levels

from which quantum-splitting processes are capable. [3-6]

## II. METHODS AND MATERIAL

$\text{MgF}_2 : \text{Gd}^{3+}, \text{Eu}^{3+}$  phosphor was synthesis via reactive atmospheric process. In this method we used metal carbonate like  $\text{MgCO}_3$ (99.99% A.R.) as a precursor. The inorganic magnesium carbonate was taken in Teflon beaker. A little amount of double distilled water was added in beaker and stired it, then hydrofluoric acid (HF) added in it to get slurry. The slurry was dried by blowing air or heating on hot plate (80°C). A freshly prepared  $\text{MgF}_2$  host was obtained.  $\text{Gd}_2\text{O}_3$  (AR 99.9%) and  $\text{Eu}_2\text{O}_3$  (AR 99.9%) were boiled in  $\text{HNO}_3$  and evaporated to dryness, so as to convert them into relevant nitrates. The aqueous

solution of these nitrates where use as a dopants. The 1 mol% of gadolinium nitrate and 1mol% of europium nitrate where assorted in the host material and dehydrated completely.

The dried powder was transferred to a glass tube and about 1.0 wt. % RAP agent was added. In this process we used ammonium fluoride as a RAP agent. The tube was closed with a tight stopper and slowly heated to 500°C for 2 h. The stopper was removed and the powders were transferred to a graphite crucible pre-heated to a suitable temperature. After heating in the graphite crucible for 1 h the resulting phosphor was rapidly quenched to room temperature. Belsare *et al.* well discussed about RAP in their literature [7]. The complete process involved in the reaction was represented as a flow chart in Fig. 1.

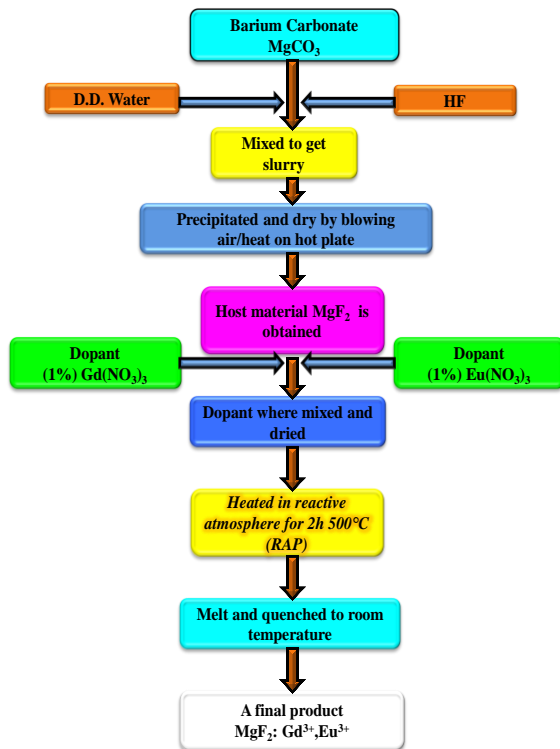


Fig.1

Fig.1. Flow chart of MgF<sub>2</sub>: Gd<sup>3+</sup>, Eu<sup>3+</sup> prepared via RAP.

Fig.2.XRD patterns of MgF<sub>2</sub>: Gd<sup>3+</sup>, Eu<sup>3+</sup> synthesized by RAP.

### III. RESULTS AND DISCUSSION

#### 3.1 XRD Analysis

The formation of the MgF<sub>2</sub>: Gd<sup>3+</sup>, Eu<sup>3+</sup> sample in the crystalline phase synthesized by RAP was confirmed by XRD pattern as shown in Fig.2. The XRD pattern for MgF<sub>2</sub>:Gd<sup>3+</sup>, Eu<sup>3+</sup> agreed well with the standard data from ICDD file (01-070-8282). Also the XRD pattern show that MgF<sub>2</sub> lattice possesses Tetragonal structure with a space group *P42/mnm(136)* with lattice parameters  $a = b = 4.5964 \text{ \AA}$  and  $c = 3.0376 \text{ \AA}$  and interfacial angles  $\alpha = \beta = \gamma = 90^\circ$ . XRD pattern of MgF<sub>2</sub>:Gd<sup>3+</sup>, Eu<sup>3+</sup> phosphor as shown in fig.1.

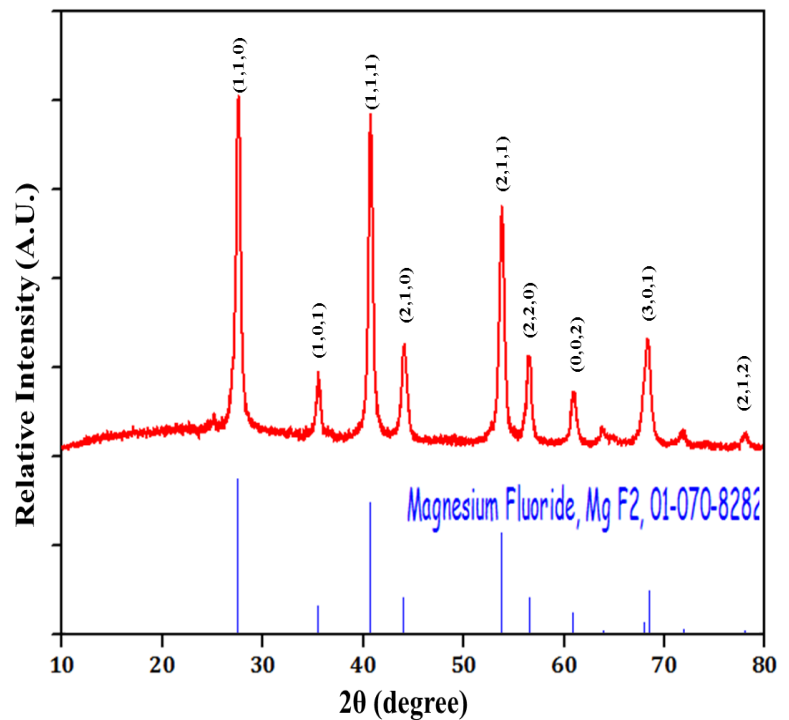


Fig.2

### 3.2 VUV-UV PL Analysis

The concentration quenching of  $Gd^{3+}$  as a sensitizer in  $MgF_2$  host background was resolute. From the Fig.3 it can be encouraged that at 1 mol% of  $Gd^{3+}$  ions in  $MgF_3$  host shows optimum intensity peak at 311 nm under the excitation of 273 nm. The emission spectra under excitation 273 and 203 nm are shown in Fig 5. The emission lines of  $Eu^{3+}$  peaked at about 593, 613, 650 and 700nm correspond to  ${}^5D_0 \rightarrow {}^7F_J$  ( $J=1, 2, 3, 4$ ) transitions respectively and the  ${}^5D_J$  ( $J=0, 1, 2, 3$ )  $\rightarrow {}^7F_J$  transition peaks of  $Eu^{3+}$  are much weaker than those of  ${}^5D_0 \rightarrow {}^7F_J$  transition. There are broad excitations lines spectra peaking optimum at about 203, 227 and 274 nm responsible for  ${}^8S_{7/2} \rightarrow {}^6G_J$ ,  ${}^6D_J$ ,  ${}^6I_J$  respectively [8] as shown in Fig 4.

The process transfer of energy and quantum splitting can happen by the combination of  $Gd^{3+}$  and  $Eu^{3+}$  in which  $Gd^{3+}$  and absorbing a VUV photon

corresponding to  ${}^8S_{7/2} \rightarrow {}^6G_J$ . The incident high energy photon is cut into two visible photons emitted by  $Eu^{3+}$  ions. The energy of transitions  ${}^6G_J \rightarrow {}^6P_J$  on  $Gd^{3+}$  matches the  ${}^7F_J \rightarrow {}^5D_0$  excitation energy on  $Eu^{3+}$ . Upon excitation in the  ${}^6G_J$  levels of  $Gd^{3+}$  as the first step, energy is transferred by cross-relaxation between  $Gd^{3+}$  and  $Eu^{3+}$  which make  $Gd^{3+}$  fall into the  ${}^6P_J$  state and  $Eu^{3+}$  is excited into the  ${}^5D_0$  state. The excited  $Eu^{3+}$  is responsible for the first visible photon. The first step is called as booming energy migration. In the second step the remaining excitation energy of  $Gd^{3+}$  in the  ${}^6P_J$  state is transferred to another nearing  $Eu^{3+}$  ion, i.e.  $Eu^{3+}$  ion exciting into a high state. Then a fast relaxation from a high excited state to  ${}^5D_J$  states will occur. After the first step, because the  $Eu^{3+}$  ion only excited into  ${}^5D_0$  state, only the emissions of  ${}^5D_0 \rightarrow {}^7F_J$  transitions are expected. However after the second step, all levels of  ${}^5D_{3,2,1,0}$  of  $Eu^{3+}$  are probably engaged, so the emission wavelength consists of all of the  ${}^5D_J$  ( $J=0,1,2,3$ )  $\rightarrow {}^7F_J$  transitions [9].

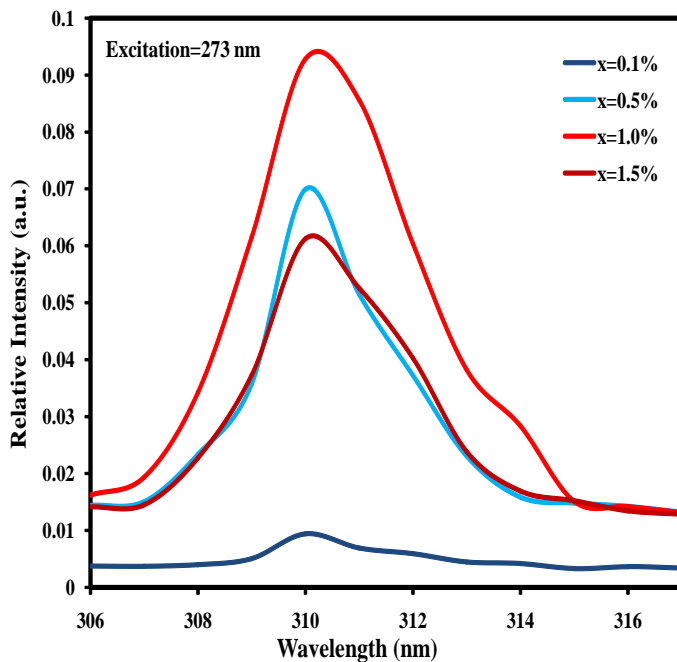


Fig.3

Fig.3.Emission spectra of  $MgF_2: X\%Gd^{3+}$  under the excitation of 273 nm.

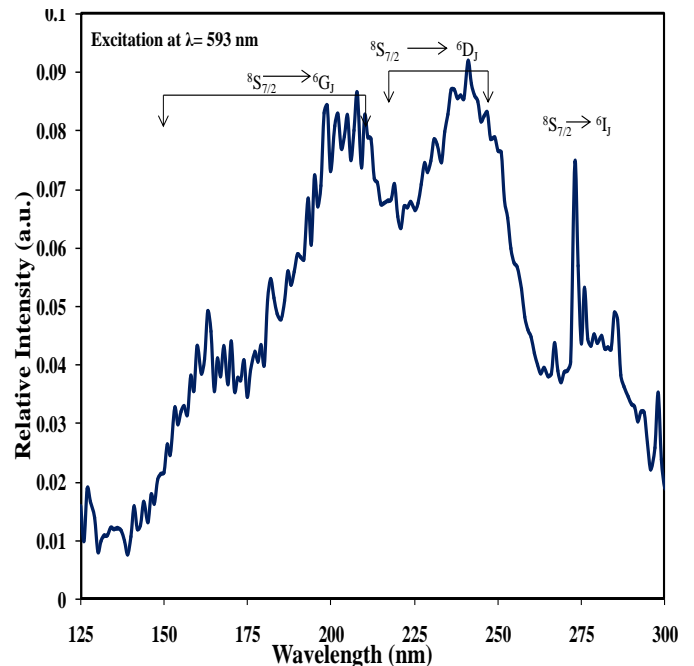


Fig.4

Fig.4.Excitation spectrum of  $MgF_2: Gd^{3+}, Eu^{3+}$  monitored at 593 nm.

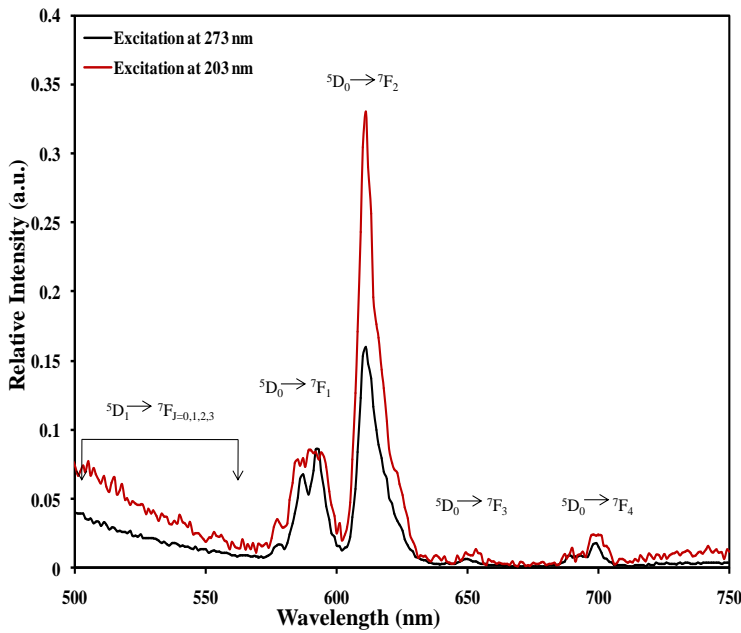


Fig.5

Fig.5. Emission spectra of MgF<sub>2</sub>: Gd<sup>3+</sup>, Eu<sup>3+</sup> at excitation wavelength 203 and 274 nm.

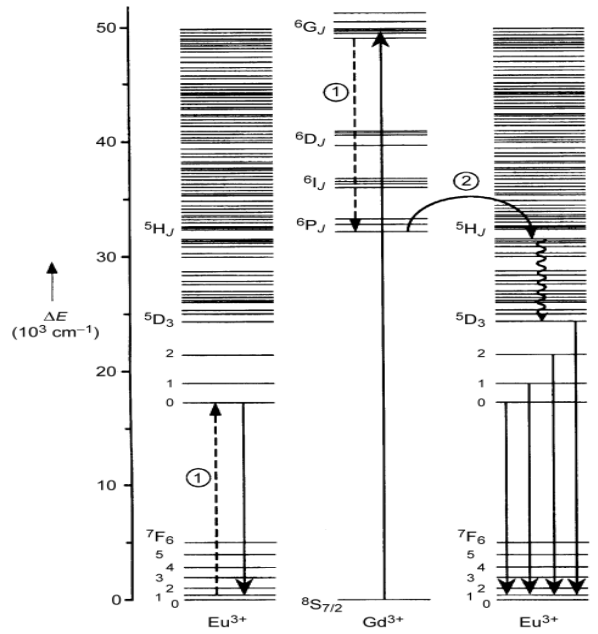


Fig.6

Fig.6. Energy level diagrams of Eu<sup>3+</sup> and Gd<sup>3+</sup> showing the cross-relaxation energy transfer process that leads to quantum splitting [9, 10]

Consecutively to calculate quantum efficiency, some assumption must be projected. The incident vacuum ultraviolet photon absorption efficiency cannot be taken into consideration. Some nonradiative losses at defects and impurities are disregarded. In the MgF<sub>2</sub>:Gd<sup>3+</sup>, Eu<sup>3+</sup> sample, different excitations are adopted including the excitation of Gd<sup>3+</sup> → <sup>6</sup>G<sub>J</sub> with 203 nm and the excitation of Gd<sup>3+</sup> → <sup>6</sup>I<sub>J</sub> with 273 nm. Upon excitation in <sup>6</sup>I<sub>J</sub> level with 273 nm, the quantum cutting never occurs because no cross-relaxation exists, so the <sup>5</sup>D<sub>J</sub> → <sup>7</sup>F<sub>J</sub> transitions emission of Eu<sup>3+</sup> has a normal branching ratio between <sup>5</sup>D<sub>0</sub> and <sup>5</sup>D<sub>1,2,3</sub>. Upon 203 nm excitation in <sup>6</sup>G<sub>J</sub> level with, the quantum cutting can occur via two-step energy transfer. In the second step, the emission of Eu<sup>3+</sup> has a normal branching ratio. The first step will pilot to the increase of <sup>5</sup>D<sub>0</sub> emission. So the ratio of <sup>5</sup>D<sub>0</sub> and <sup>5</sup>D<sub>1,2,3</sub> emissions is expected to increase. To determine the efficiency of the cross relaxation, the formula proposed by Wegh [11-20] was adopted as follows:

$$\frac{P_{CR}}{P_{CR} + P_{DT}} = \frac{R(^5D_0/^5D_{1,2,3})_{6G_J} - R(^5D_0/^5D_{1,2,3})_{6I_J}}{R(^5D_0/^5D_{1,2,3})_{6I_J} + 1}$$

Where P<sub>CR</sub> is the probability for cross-relaxation, P<sub>DT</sub> is the probability for the direct transfer from Gd<sup>3+</sup> to Eu<sup>3+</sup>. R (<sup>5</sup>D<sub>0</sub>/<sup>5</sup>D<sub>1, 2, 3</sub>) is the ratio of the <sup>5</sup>D<sub>0</sub> and <sup>5</sup>D<sub>1, 2, 3</sub> emission integral intensities. The subscript (<sup>6</sup>G<sub>J</sub> or <sup>6</sup>I<sub>J</sub>) represents the excitation level for which the ratio is observed. From the emission spectra, the value of R (<sup>5</sup>D<sub>0</sub>/<sup>5</sup>D<sub>1, 2, 3</sub>)<sub>6G<sub>J</sub></sub> and (<sup>5</sup>D<sub>0</sub>/<sup>5</sup>D<sub>1, 2, 3</sub>)<sub>6I<sub>J</sub></sub> can be calculated 44.12 and 29.42, respectively. Therefore, the value of P<sub>CR</sub>/P<sub>CR</sub> + P<sub>DT</sub> is 0.32. It means that there are 32% Gd<sup>3+</sup> ions in the <sup>6</sup>G<sub>J</sub> excited state settle down through a two-step energy transfer emitting two visible photons in this method. So the quantum cutting efficiency of 132% can be obtained. Quantum cutting in the Gd to Eu understanding requires energy transfer over the Gd sublattice to Eu [10].

#### IV. CONCLUSION

The inorganic material  $\text{MgF}_2: \text{Gd}^{3+}, \text{Eu}^{3+}$  was successfully prepared through reactive atmosphere process. The XRD pattern confirmed its cubic structure. The visible quantum cutting and energy transfer through down-conversion was observed in  $\text{MgF}_2: 1\% \text{Gd}^{3+}, 1\% \text{Eu}^{3+}$  and the quantum efficiency was found to be around 132% under the excitation of 203 nm equivalent  $^8\text{S}_{7/2} \rightarrow ^6\text{G}_J$  transition of  $\text{Gd}^{3+}$  ions.

#### V. ACKNOWLEDGEMENTS

We are thankful to 4B8 VUV spectroscopy beam line scientists of Beijing Synchrotron Radiation Facility (BSRF), China for given that access in recording VUV on beamline 4B8 under dedicated synchrotron mode using remote access mode. One of the authors S.R. Jaiswal thankful to Head, Department of Physics SantGadge Baba Amravati University, Amravati for providing necessary facilities.

#### VI. REFERENCES

- [1]. C.R. Ronda, J. Alloys Compd. 225 (1993) 534.
- [2]. M. Y. William, Phosphor Handbook, CRC press is an imprint of the Taylor & Francis Group, ISBN: 0-8493-3564-7.
- [3]. S. Pote, C. Joshi, S. Moharil, P. Muthal, S. Dhopte. ISSN 1061-3862, International Journal of Self- Propogating High-Temperature Synthesis. 22 (2013) 37-40
- [4]. B. Herden, A. García-Fuente, H. Ramanantoanina, T. Jüstel, C. Daul, W. Urland, Chemical physics letter. 620 (2015) 29-34.
- [5]. W. Binder, S. Dislerhoff, J. Cameron, Dosimetric Properties of  $\text{CaF}_2: \text{Dy}$ , (a) Proc. II Int. Conf. on Lumin. Dosim., Gatlinberg, 1968, pp. 45–53; (b) Health Phys., 1969, vol. 17, no. 4, pp. 613–618.
- [6]. (a) A.C. Lucas, R.H. Moss, B.M. Casper, Thermoluminescent  $\text{CaF}_2: \text{Tm}$  and Method for Its Use, US Patent 4 039 834, 1977; (b) Lucas, A.C. and Casper, B.M., Thermoluminescence of Thulium Doped Calcium Fluoride, Proc. Int. Conf. on Lumin. Dosim., Sao Paulo (Brazil), 1977, pp. 131-139
- [7]. P. Belsare, C. Joshi, S. Moharil, V. Kondawar, P.Muthal, S. Dhopte, J. Alloys Compd. 450 (2008) 468–472.
- [8]. R.T. Wegh, E.V.D. van Loef, A. Meijerink, J. Lumin., 90 (2000) 111.
- [9]. B. Liua, Y. Chena, C. Shia, H. Tanga, Y. Tao, Journal of Luminescence 101 (2003) 155–159.
- [10]. R.T. Wegh, H. Donker, K. Oskam, and A. Meijerink, J. Lumin., 82 (1999) 93.
- [11]. R.T. Wegh, H. Donker, K. Oskam, A. Meijerink, Science 663 (1999) 283.
- [12]. N. Kodama, Y. Watanabe, Appl. Phys. Lett. 4141 (2004) 84.
- [13]. N. Kodama, S. Oishi, J. Appl. Phys. 103515 (2005) 98.
- [14]. R. Hua1, J.H. Niu, B.J. Chen, M.T.Z. Li, T. Yu, W.L. Li, Nanotechnology 1642 (2006) 17.
- [15]. Y. Zhou, S.P. Feofilov, J.Y. Jeong, D.A. Keszler, R.S. Meltzer, Phys. Rev. B 075129 (2008) 77.
- [16]. M. Karbowski, A. Mech, W. Ryba-Romanowski, J. Lumin. 65 (2005) 114.
- [17]. B. Liu, Y.H. Chen, C.S. Shi, H.G. Tang, Y. Tao, J. Lumin. 101 (2003) 155.
- [18]. S.K. Omanwar, S.R. Jaiswal, P.A. Nagpure, V. B. Bhatkar, J. Material Sci.: Material in Electronic(2016) 1-8
- [19]. S.K. Omanwar, S.R. Jaiswal, N.S. Sawal, K.A. Koparkar P.A. Nagpure, V. B. Bhatkar, St. petrbergpolytechnicaluniversityJournal : Physics and mathematics 3 (2017) 218-224.
- [20]. S.R. Jaiswal, N.S. Sawal, K.A. Koparkar, V. B. Bhatkar, S.K. Omanwar, material discovery, 7 (2017) 15-20.